Conducting Materials

International Edition: DOI: 10.1002/anie.201502498
German Edition: DOI: 10.1002/ange.201502498

A Single-Step Synthesis of Electroactive Mesoporous ProDOT-Silica Structures**

Jeonghun Kim, Byeonggwan Kim, Chokkalingam Anand, Ajayan Mano, Javaid S. M. Zaidi, Katsuhiko Ariga, Jungmok You, Ajayan Vinu, and Eunkyoung Kim**

Abstract: *The single-step preparation of highly ordered mesoporous silica hybrid nanocomposites with conjugated polymers was explored using a novel cationic 3,4-propylenedioxythiophene (ProDOT) surfactant (PrS). The method does not require high-temperature calcination or a washing procedure. The combination of self-assembly of the silica surfactant and in situ polymerization of the ProDOT tail is responsible for creation of the mesoporosity with ultralarge pores, large pore volume, and electroactivity. As this novel material exhibits excellent textural parameters together with electrical conductivity, we believe that this could find potential applications in various fields. This novel concept of creating mesoporosity without a calcination process is a significant breakthrough in the field of mesoporous materials and the method can be further generalized as a rational preparation of various mesoporous hybrid materials having different structures and pore diameters.*

Mesoporous materials (MMs) have attracted much attention because of their applications in the fields of adsorbent, catalysis, fuel cells, and nanostructured templates.[1] In the synthetic process for mesoporous silica, surfactants play a critical role in controlling morphology, pore size, surface area, and dimensions.[2] Various types of surfactants, including cationic, anionic, non-ionic, and lizard, have been used to create MMs having a well-controlled pore structure (hexagonal, cubic, etc.) with high specific surface area and pore volume.[3] Researchers also tried to provide fluorescent conjugated polymer (CP)-silica MMs.[4] Unfortunately, the pores of the materials are not accessible and mostly filled by surfactants with CPs. As these organic surfactants are used as pore-forming agents, these molecules should be removed either by calcination or washing with an HCl/ethanol mixture to obtain the porous structure. This step is one of the major disadvantages of the hydrothermal sol–gel technique because removal of the surfactant molecules at the final stage of the fabrication of MMs presents a major hurdle for the commercialization of these exciting materials. Thus it is critical to find an easy method for the preparation of functional MMs without any calcination treatment.

Herein we demonstrate for the first time, the single-step preparation of highly ordered and electrically conductive polymer-silica hybrid MMs (PSM-1) by using in situ polymerization and the novel cationic surfactant PrS (Figure 1). We introduced a polymerizable 3,4-propylenedioxythiophene (ProDOT) group to PrS to create conductive network within PSM-1 (Figure 1; see Section S1 in the Supporting Information). The new PrS, having a bulky hydrophobic end group, provides not only larger volume but also supports the enlargement of the pore size of the MMs. As prepared, PSM-1 is highly ordered with porous hexagonal structures and, most importantly, the textural parameters such as pore volume and diameter are similar to the well-known silica MMs, such as SBA-15, KIT-6, and KIT-5, which are prepared at 100 °C. In addition, the wall structure of PSM-1 contains aromatic CP units which are electrically active and offer conductivity which is much higher than that of insulating mesoporous silica (see Table S2).

Generally, the length and the volume of the hydrophobic alkyl chain, of either anionic or cationic surfactants, in the synthetic mixture dictate the pore diameter and the pore volume of the MMs.[3d–f] However, the use of the long-chain surfactants always results in a decrease of structural order because of the mismatches in the surfactants head-to-tail packing ratio. In contrast, the introduction of large amounts of swelling agents for pore-size enlargement during the synthesis is not an appropriate method for industrial scale synthesis because it requires an additional process for separation and recycling of the swelling agent. These large

---

[*] Dr. J. Kim,[+] Dr. B. Kim,[+] Dr. J. You, Prof. Dr. E. Kim
Department of Chemical and Biomolecular Engineering
Active Polymer Center for Pattern Integration
Yonsei University
50 Yonsei-ro, Seodaemun-gu, Seoul 120-749 (South Korea)
E-mail: eunkim@yonsei.ac.kr

Dr. C. Anand, Dr. J. S. M. Zaidi, Prof. Dr. A. Vinu
Australian Institute for Bioengineering and Nanotechnology
University of Queensland, Brisbane, Queensland 4072 (Australia)
E-mail: a.vinu@uq.edu.au

Dr. A. Mano, Dr. K. Ariga, Prof. Dr. A. Vinu
International Center for Materials Nanoarchitectonics
National Institute for Materials Science (NIMS)
1-1 Namiki, Tsukuba 305-0044, Ibaraki (Japan)

[+] These authors contributed equally to this work.

[**] This work was financially supported by the Ministry of Education, Culture, Sports, Science and Technology (MEXT) under the Strategic Program for Building an Asian Science and Technology Community Scheme and WPI Initiative on Materials Nanoarchitectonics, MEXT (Japan). J.K. thanks NIMS for offering IJGS Fellowship. E.K. also acknowledges the financial support of the National Research Foundation of Korea (NRF) funded by the Korea government (MSIP) (2007-0056091 and 2010-0019313). A.V. also thanks the Australian Research Council for the Future Fellowship, the University of Queensland for the start-up grant, and the Alexander von Humboldt-Foundation for the Friedrich Wilhelm Bessel Award. Current affiliation of Prof. J. You is the Department of Plant & Environmental New Resources, Kyung Hee University, Republic of Korea.

Supporting information for this article is available on the WWW under http://dx.doi.org/10.1002/anie.201502498.

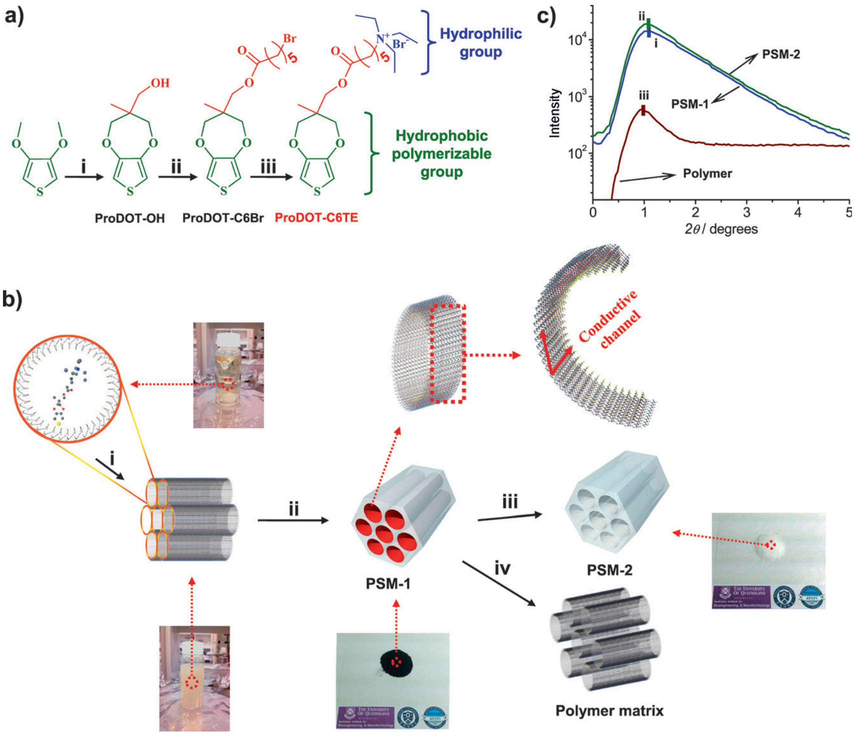

Figure 1. Synthesis of ProDOT-C6TE and the conductive mesoporous silica hybrid composite with ultralarge pores, as well as the FT-IR and SAXS characterizations of the materials. a) Synthesis of the novel cationic surfactant ProDOT-C6TE. i) reflux, 80% yield; ii) R.T. 94.5% yield; iii) reflux, 97% yield. b) The preparation of PSM-1 and the pure mesoporous silica using ProDOT-C6TE. i) Micelle formation; ii) condensation of TEOS and the polymerization of PrS; iii) calcination at 540 °C in air; and iv) HF (aq) treatment (see details in the Supporting Information). c) SAXS patterns of PSM-1 (blue), PSM-2 (green), and the pure CP matrix (brown). The bars indicate the pore diameters of i) 7.8, ii) 8.5, and iii) 9.2 nm.

hydrophobic end groups help to organize the micelles, having an empty volume at the center, and are responsible for the large pore size of the MMs.

A new PrS was synthesized from 3,4-dimethoxythiophene over three steps (see Section S1).[5] The synthesized ProDOT-C6TE showed N–C stretching at 1022 cm^{-1} and all materials showed the C–H stretching from the 2,5-positions of the thiophene group at 3105–3109 cm^{-1} (see Figure S2 and Table S1). PSM-1 was synthesized quantitatively through self-assembly (SA) and the in situ polymerization of PrS and sol-gel reaction of tetraethyl orthosilicate (TEOS), which is used as a silica source under acidic conditions. It is interesting to note that the color of the synthesis mixture changed from clear light-yellow to black when the reaction mixture was treated at 100 °C, thus revealing the oxidative polymerization and the SA of the surfactant with TEOS. The resultant PSM-1 was treated with HF(aq) to obtain the pure polymer matrix without silica. To obtain the pure silica MM (PSM-2), PSM-1 was calcined at 540 °C for 24 hours. The successful synthesis of the CP-silica hybrid composite was confirmed by FTIR and MALDI-TOF (see Section S2).[6,7]

In the small-angle X-ray scattering (SAXS) patterns, PSM-1 and PSM-2 exhibited strong and high-intensity peaks with similar scattering vectors, which can be indexed to the hexagonal space-group p6m (Figure 1c). These results indicate that PSM-1 and PSM-2 are highly ordered and similar to the SBA-15 prepared from the non-ionic surfactant. Interestingly, the polymer also exhibited a strong peak with a large interplanar distance of 9.2 nm. It must be noted that the pure polymer sample was not soluble in any solvents, thus indicating the formation of insoluble CPs with enough chain length for conductivity. After calcination, the color of PSM-1 changed from black to white and the total weight loss after the calcination was calculated to be about 9.88% because of the burning out of the organic materials (see Figure S3). The chemical composition of PSM-1 was measured from elemental analysis (EA), SEM-EDX, and ToF-SIMS (Figure 2a; see Figures S4 and S5). The composition of the organic matter by EA was about 12%, which is similar with TGA data. More Cl^- ions were detected than Br^- ions, based on both SEM-EDX mapping and ToF-SIMS spectra, because the ammonium chloride bond is more stable than ammonium bromide bond.[8] Therefore, ammonium chloride was left in the final product by the ion-exchange process. Also, the EDX mapping images showed uniformly dispersed C, H, N, O, S, Si, Cl, and Br elements at the PSM-1 particles, thus indicating successful synthesis of PSM-1. The HRTEM images of PSM-1 showed highly ordered mesopores which are arranged in a regular interval (Figure 2c–e), thus confirming that mesopores are generated through the combination of the SA process of the ProDOT-C6TE. To the best of our knowledge, this is the first report on the fabrication of conductive mesoporous hybrid silica composite, having a well-ordered mesoporous structure, in a single step without any calcination or a washing procedure.

The textural parameters of the PSM-1 before and after calcination were obtained by a nitrogen adsorption-desorption isotherm.[9] Both samples show a type IV adsorption isotherm with a sharp capillary condensation step and H1-type hysteresis loop, which is a characteristic of well-ordered MMs (Figure 3a). The capillary condensation step of the sample occurred at a relative pressure higher than 0.7, thus indicating the presence of large mesopores in the samples. The PSM-1 exhibits a total NLDFT pore volume of 0.68 $cm^3 g^{-1}$ and the BET specific surface area of 337 $m^2 g^{-1}$ (Table S3). The NLDFT pore-size distribution data reveal that the pores are highly uniform with a maximum size of about 7.8 nm. It is quite surprising that the material showed excellent textural characteristics with a large-pore diameter even before the calcination. For the first time porosity with excellent textural characteristics is observed for the uncalcined sample. The capillary condensation step for the PSM-2 is shifted towards a higher relative pressure, thus indicating an enlargement in the pore size after the calcination. This

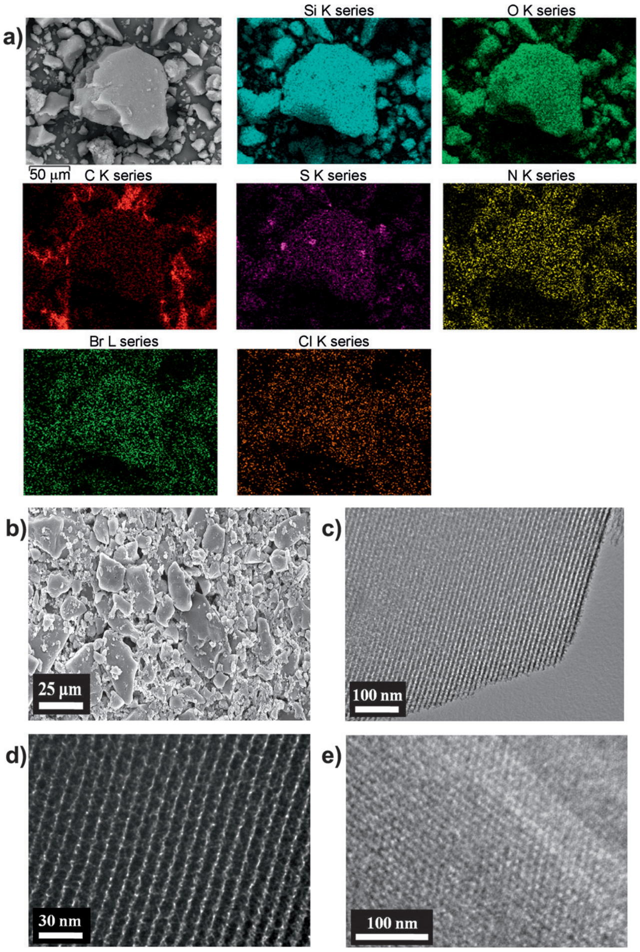

Figure 2. Electron microscopic investigation on PSM-1. a) SEM energy dispersive X-ray spectroscopy (EDX) elemental mapping images of PSM-1. b) A HRSEM image of PSM-1. c–e) HRTEM images of PSM-1. The HRSEM image shows a planar-shapelike morphology of PSM-1 and HRTEM images showed the highly ordered mesoporous structure with an ultralarge pore of about 10 nm.

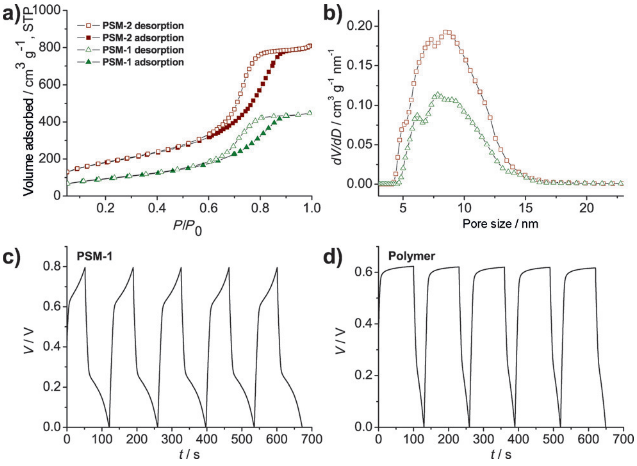

Figure 3. Pore structure analysis of the PSM-1 and PSM-2, and charge/discharge curves for the PSM-1 and polymer. a) N_2 adsorption-desorption isotherms of PSM-1 (green) and PSM-2 (red). b) Pore-size distributions of PSM-1 (green) and PSM-2 (red) calculated from the adsorption branch of the isotherms. Galvanostatic charge/discharge curves of c) PSM-1 and d) polymer (HF treated). Potentials were cycled from 0 to 0.8 V within 100 s cycle at a constant current of 1.2 µA in an aqueous solution of 0.1 м HCl.

enlargement is mainly due to the removal of the organic moieties from the hybrid material through the oxidation during the high-temperature calcination process under air. The BET specific surface area and the NLDFT specific pore volume of the PSM-2 are 655 $m^2 g^{-1}$ and 1.22 $cm^3 g^{-1}$, respectively, and are much larger than those of the uncalcined PSM-1 sample. After the calcination process, PSM-2 exhibited well-ordered porous structure with a large pore volume and uniform pore size which demonstrates that the structure of the material is quite stable, even after the removal of conductive organic part. The mechanism for the formation of mesoporosity in the uncalcined PSM-1 is schematically shown in Figure S7.

At first we compared the SA process of silica with dodecyltriethyl ammonium bromide and PrS as the chain length of the hydrophobic tail of both surfactants is almost same. PrS has a bulky cyclic dioxyalkylene group, ProDOT, as a tail group and an alkyl group connected to the large head group, triethylammonium bromide. Although the surfactant has a short alkyl chain, the molecules self-assembled in a $S^+ X^- I^+$ fashion [cationic surfactants (S^+), halogen anions (X^-) and cationic silicic acid species (I^+)]. Since the tail group is bulky, the SA process of PrS is quite different from that of dodecyltrimethyl ammonium bromide. In the case of PrS, the large tail group serves as a swelling agent, such as 1,3,5-trimethylbenzene which is generally used in the synthesis of large-pore mesoporous silica for enhancement of pore size, and creates a void space at the center of the micelles. This tail group is one of the reasons for the generation of the large pore in the uncalcined sample. We also surmise that when the synthesis temperature is increased, the polymerization of the ProDOT tail group with the neighboring ProDOT may be initiated by deprotonation[10] due to the existence of H^+ ions in the reaction mixture and high temperatures, which might change the orientation of the individual PrS molecules from vertical to horizontal. This change in orientation might enlarge the micelles and create a large void space at the center of the micelles. In addition, we carried out a dynamic light scattering (DLS) study on the monomer as shown in Figure S6. We examined the aqueous solution under the same conditions as that for PSM-1, and compared the result with cetyltrimethylammonium bromide (CTAB), which is a simple cationic ammonium surfactant. Assuming that a micelle of the surfactant has a spherical shape, the size of the micelle is calculated to be about 200 nm in diameter, which is much larger than that of the CTAB. Furthermore, the size distribution of the surfactant was not changed, even after 2 days, to within a 5 % error, thus confirming that the micelle of the surfactant is highly stable during the reaction. At present, we feel that this is only the possible mechanism for the formation of large mesopores in the uncalcined sample. Another exciting feature of the PSM-1 is the electrical conductivity along the wall structure composed of silica and the polymeric form of PrS (see Table S2). The PSM-1 samples showed electrical conductivity of 2.7×10^{-6} and 2.5×10^{-5} $S\,cm^{-1}$, before and after I_2 doping, respectively. The conductivity values were decreased in the PSM-2 after HF treatment. It may be due to the highly ordered polymer-silica composite structure, in which electrical transport may be hampered by the large pores. Interestingly, when PSM-1 was doped with *p*-toluenesulfonic acid, the conductivity was significantly increased (9.0×10^{-4} S cm^{-1}).

Similarly, the pure polymer sample showed a large increase in conductivity upon doping. As most of the polythiophenes show increased conductivity upon doping, and such a conductivity increase from that of PSM-1 and silica-free polymeric samples strongly suggest the presence of conductive channel originating from the surfactant. Notably, these conductivity values are high in the bulk-state materials compared to those of thin-film materials,[11] and importantly improved in MM composites. In contrast, the electrical conductivity of the PSM-2 or typical mesoporous silica samples were not measurable from the four-point probe method as it is beyond detection range (ca. 10^{-10} S cm^{-1}). From the FTIR data and high electrical conductivity it could be concluded that PrS was polymerized under strongly acidic conditions. Although the conductivity of PSM-1 is somewhat lower than that of the chemically polymerized polythiophenes (10^{-3}–10^{-4} S cm^{-1}), the material is still very attractive as they possess well-ordered porous structure and can be prepared in a single synthetic step.

By taking advantage of the electrical activity of PSM-1, we were able to assemble a supercapacitor, which showed characteristic charge/discharge curves (Figure 3 c,d). The specific capacitance (C_{sp}) was determined by using the equation of $C_{sp} = It_d/m_e$, where I is the applied current to the active electrode, t_d is the discharging time, and m_e is the mass of electrode material. The value of the specific capacitance for the capacitors based on PSM-1 (0.22 F g^{-1}) was four times larger than that of the HF treated polymer (0.051 F g^{-1}). Although the C_{sp} of PSM-1 was lower compared to that of CP films, possibly because of the difference in density as well as conductivity between the samples, this new approach in preparation of electroactive hybrid materials has a high potential for applications in electrical devices in future.

In conclusion, we demonstrate the preparation of novel highly ordered mesoporous silica hybrid materials, having a large pore size, without any calcination or washing treatment. The combination of the SA of the polymerizable surfactant and the silica species, and the polymerization of the tail group of the surfactant molecules creates a well-ordered porosity, even in the uncalcined samples. The obtained materials not only exhibit the excellent textural parameters but also offer a high conductivity. We strongly believe that this novel methodology represents a breakthrough in the field of MMs. In addition, this method can be extended to the fabrication of various mesoporous hybrid materials using new surfactant molecules, and creates a platform for the generation of hybrid MMs. These electrically conductive polymer-silica hybrid MMs could also find potential applications in various fields, including fuel cells, sensors, organic devices, and drug delivery systems.

Keywords: conducting materials · mesoporous materials · polymers · self-assembly · surface analysis

How to cite: *Angew. Chem. Int. Ed.* **2015**, *54*, 8407–8410
Angew. Chem. **2015**, *127*, 8527–8530

---

[1] a) J. Y. Ying, C. P. Mehnert, M. S. Wong, *Angew. Chem. Int. Ed.* **1999**, *38*, 56–77; *Angew. Chem.* **1999**, *111*, 58–82; b) B. G. Trewyn, C. M. Whitman, V. S. Y. Lin, *Nano Lett.* **2004**, *4*, 2139–2143.

[2] a) G. J. d. A. A. Soler-Illia, C. Sanchez, B. Lebeau, J. Patarin, *Chem. Rev.* **2002**, *102*, 4093–4138; b) Y. Wan, D. Zhao, *Chem. Rev.* **2007**, *107*, 2821–2860; c) C. T. Kresge, M. E. Leonowicz, W. J. Roth, J. C. Vartuli, J. S. Beck, *Nature* **1992**, *359*, 710–712.

[3] a) J. S. Beck, J. C. Vartuli, W. J. Roth, M. E. Leonowicz, C. T. Kresge, K. D. Schmitt, C. T. W. Chu, D. H. Olson, E. W. Sheppard, *J. Am. Chem. Soc.* **1992**, *114*, 10834–10843; b) Q. Huo, D. I. Margolese, U. Ciesla, P. Feng, T. E. Gier, P. Sieger, R. Leon, P. M. Petroff, F. Schuth, G. D. Stucky, *Nature* **1994**, *368*, 317–321; c) S. Che, A. E. Garcia-Bennett, T. Yokoi, K. Sakamoto, H. Kunieda, O. Terasaki, T. Tatsumi, *Nat. Mater.* **2003**, *2*, 801–805; d) Q. Huo, R. Leon, P. M. Petroff, G. D. Stucky, *Science* **1995**, *268*, 1324–1327; e) J. Tang, J. Liu, C. Li, Y. Li, M. O. Tade, S. Dai, Y. Yamauchi, *Angew. Chem. Int. Ed.* **2015**, *54*, 588–593; *Angew. Chem.* **2015**, *127*, 598–603; f) Q. Huo, D. I. Margolese, G. D. Stucky, *Chem. Mater.* **1996**, *8*, 1147–1160.

[4] Z. Yang, X. Kou, W. Ni, Z. Sun, L. Li, J. Wang, *Chem. Mater.* **2007**, *19*, 6222–6229.

[5] a) A. Kumar, D. M. Welsh, M. C. Morvant, F. Piroux, K. A. Abboud, J. R. Reynolds, *Chem. Mater.* **1998**, *10*, 896–902; b) B. Kim, H. Shin, T. Park, H. Lim, E. Kim, *Adv. Mater.* **2013**, *25*, 5483–5489; c) T. Bhuvana, B. Kim, X. Yang, H. Shin, E. Kim, *Angew. Chem. Int. Ed.* **2013**, *52*, 1180–1184; *Angew. Chem.* **2013**, *125*, 1218–1222.

[6] a) J. Kim, J. You, E. Kim, *Macromolecules* **2010**, *43*, 2322–2327; b) J. Kim, J. You, B. Kim, T. Park, E. Kim, *Adv. Mater.* **2011**, *23*, 4168–4173.

[7] S. Garreau, G. Louarn, J. P. Buisson, G. Froyer, S. Lefrant, *Macromolecules* **1999**, *32*, 6807–6812.

[8] P. Tundo, P. Venturello, E. Angeletti, *J. Am. Chem. Soc.* **1982**, *104*, 6547–6551.

[9] E. P. Barrett, L. G. Joyner, P. P. Halenda, *J. Am. Chem. Soc.* **1951**, *73*, 373–380.

[10] a) Y. Yagci, F. Yilmaz, S. Kiralp, L. Toppare, *Macromol. Chem. Phys.* **2005**, *206*, 1178–1182; b) A. Elschner, S. Kirchmeyer, W. Lovenich, U. Merker, K. Reuter, *PEDOT: Principles and Applications of an Intrinsically Conductive Polymer*, 1st ed., CRC, Boca Raton, Fl, **2010**.

[11] A. A. Talin, A. Centrone, A. C. Ford, M. E. Foster, V. Stavila, P. Haney, R. A. Kinney, V. Szalai, F. El Gabaly, H. P. Yoon, F. Léonard, M. D. Allendorf, *Science* **2014**, *343*, 66–69.

Received: March 24, 2015